

OPEN ACCESS

High dynamic range diamond detector acquisition system for beam wire scanner applications

To cite this article: J.L. Sirvent *et al*/2016 *JINST* 11 C03008

View the [article online](#) for updates and enhancements.

Related content

- [Secondary particle acquisition system for the CERN beam wire scanners upgrade](#)
J.L. Sirvent, B. Dehning, J. Emery *et al*.
- [THE OHIO-STATE IMAGE-DISSECTOR SCANNER](#)
P. L. Byard, C. B. Foltz, H. Jenkner *et al*.
- [Residual strain in the Nb₃Sn 11 T dipole magnet coils for HL LHC](#)
C Scheuerlein, M Di Michiel, M Hofmann *et al*.



IOP | ebooks™

Bringing you innovative digital publishing with leading voices to create your essential collection of books in STEM research.

Start exploring the collection - download the first chapter of every title for free.

RECEIVED: November 15, 2015

REVISED: January 4, 2016

ACCEPTED: January 18, 2016

PUBLISHED: March 3, 2016

TOPICAL WORKSHOP ON ELECTRONICS FOR PARTICLE PHYSICS 2015,
SEPTEMBER 28TH – OCTOBER 2ND, 2015
LISBON, PORTUGAL

High dynamic range diamond detector acquisition system for beam wire scanner applications

J.L. Sirvent,^{a,b,1} B. Dehning,^a E. Piselli,^a J. Emery^a and A. Dieguez^b

^aThe European Organization for Nuclear Research (CERN),
Geneva, 1211 Switzerland

^bFacultat de Física, Universitat de Barcelona,
C. de Martí i Franquès n^o1, Barcelona, 08028 Spain

E-mail: jsirvent@cern.ch

ABSTRACT: The CERN Beam Instrumentation group has been working during the last years on the beam wire scanners upgrade to cope up with the increasing requirements of CERN experiments. These devices are used to measure the beam profile by crossing a thin wire through a circulating beam, the resulting secondary particles produced from beam/wire interaction are detected and correlated with the wire position to reconstruct the beam profile. The upgraded secondary particles acquisition electronics will use polycrystalline chemical vapour deposition (pCVD) diamond detectors for particle shower measurements, with low noise acquisitions performed on the tunnel, near the detector. The digital data is transmitted to the surface through an optical link with the GBT protocol. Two integrator ASICs (ICECAL and QIE10) are being characterized and compared for detector readout with the complete acquisition chain prototype. This contribution presents the project status, the QIE10 front-end performance and the first measurements with the complete acquisition system prototype. In addition, diamond detector signals from particle showers generated by an operational beam wire scanner are analysed and compared with an operational system.

KEYWORDS: Diamond Detectors; Front-end electronics for detector readout; Detector control systems (detector and experiment monitoring and slow-control systems, architecture, hardware, algorithms, databases); Beam-line instrumentation (beam position and profile monitors; beam-intensity monitors; bunch length monitors)

¹Corresponding author.

Contents

1	Introduction	1
1.1	The beam wire scanners upgrade program	1
1.2	Secondary shower acquisition system upgrade	2
2	Secondary shower acquisition system architecture	2
2.1	Front-end design	3
2.2	QIE10 front-end evaluation	3
2.3	ICECAL_V3 front-end functional tests	5
3	System tests with beam wire scanners	5
3.1	SPS set-up	5
3.2	Diamond detectors as beam profile monitors and QIE10 front-end performance	6
4	Conclusions	10

1 Introduction

A beam wire scan is an interceptive method for transverse beam profile measurements. The working principle of wire scanners consists on the passage of a very thin carbon wire ($\sim 30\mu\text{m}$) through the particle beam. The secondary particle shower generated by the beam/wire interaction, is detected outside of the beam pipe and transformed into an electrical current proportional to the loss intensity. The beam profile is reconstructed by plotting the loss intensity versus the wire position. Using the measurements from these devices the beam is determined, allowing the calculation of the beam emittance, an important parameter for optimizing collider's luminosity.

1.1 The beam wire scanners upgrade program

The CERN accelerator complex currently has 32 installed beam wire scanner systems of different architectures located along the injector chain and in the Large Hadron Collider (LHC) itself. In terms of mechanics, these systems share some common characteristics, such as the transfer of the motor movement from air to vacuum through bellows. These bellows have a limited lifetime and have compromised accelerator operation in the past through the appearance of vacuum leaks. In addition, the use of complex mechanics leads to mechanical play that reduces the systems accuracy and hence measurement performance. The current scan speeds are also limited and do not allow the measurement of high intensity beams due to wire sublimation [1].

The development of a new scanner type is motivated by all the above mentioned issues and the need to measure smaller beam sizes at higher intensities in the future. The basic concept is to combine a high scan velocity, nominally 20ms^{-1} to avoid wire damage, with an accurate and direct wire position determination avoiding bellows and any lever arm mechanism. The specified beam

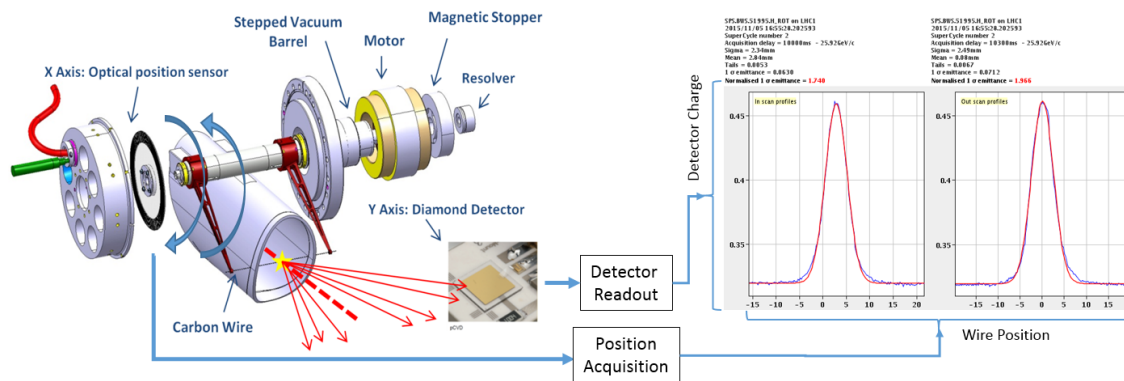


Figure 1. Upgraded beam wire scanner design and working principle.

profile measurement accuracy is set to $2\mu\text{m}$. The upgraded system, common for the CERN PSB, PS, SPS and LHC, is therefore based on an in-vacuum motor rotor, with the stator outside. This new architecture avoids the use of bellows, and incorporates an optical position sensor for accurate wire position determination [2] (see figure 1).

1.2 Secondary shower acquisition system upgrade

Presently, the secondary particle showers from operational beam wire scanners are detected by a scintillator. The light produced transits a wheel of selectable optical filters, then, a photo multiplier tube (PMT) transforms the optical signal into a current. A current-to-voltage (transimpedance) amplifier is used to drive the signal over CK50 coaxial cables, of up to 250m, to surface buildings where the digitalization is performed. To reach a suitable resolution, this architecture obliges the accelerator operators to set-up the system, selecting a suitable combination of PMT gain and optical filter according to the beam characteristics. On these systems the dynamic range is limited by the pre-amplifier, sometimes the Gaussian tails of the beam profile are too much shadowed by noise, and in some cases PMT saturation effect can lead to incorrect measurements [3].

The upgraded secondary shower acquisition system aims to use 500um thick polycrystalline chemical vapour deposition (pCVD) diamond as detector. This requires new acquisition electronics which need to cover the high dynamic range of the diamond detector without tuneable parameters, while also providing very low noise measurements. The design of such system must be compatible with any CERN accelerator and beam wire scanner location.

2 Secondary shower acquisition system architecture

A previous article describes the motivation behind the architecture choice [4]. A custom radiation tolerant front-end has been designed to resist a total ionization dose (TID) of 1KGy over the operational life of the system (10 years with an estimated TID of 100Gy/year). This front-end will be placed in the tunnel at $\sim 10\text{m}$ from the diamond detector. The front-end will perform charge integrations at 40MHz, synchronous with the beam and with a very high dynamic range. To reach the required dynamic range, the diamond detector signal will be splitted on two or four lines at different gains and acquired in parallel on the front-end. The digital data will be sent to the

back-end electronics through a dual single mode optical fibre using the CERN's GBT protocol at 4.8Gbps [5]. The front-end synchronization, data transmission and control are performed through the optical link. For the back-end system, the CERN custom designed VME FMC Carrier board (VFC-HD) [6] will be used to manage the data processing and storage. On the VFC-HD, one Small Form-Factor Pluggable (SFP+) transceiver is needed per system, allowing up to 4 front-ends to be controlled with a single board.

2.1 Front-end design

For the detector readout, two integrator ASIC candidates are being evaluated, ICECAL [7], and QIE10 [8]. For a fast evaluation, the digital front-end was designed in a modular way. On the first prototype development, the Igloo2 UMD Mezzanine [9] from the CERN CMS collaboration is used as a digital motherboard, responsible for driving the optical link. This board features an Igloo2 flash-based FPGA with the GBT protocol implemented on its firmware and a versatile link transceiver (VTRx). On future front-end versions this board will be substituted by a GBTx-based board (GEFE) [10] for enhanced radiation tolerance.

Independent mezzanine boards, for each of the two readout ASIC candidates, were designed to be attached to the motherboard through a SAMTEC connector. The two front-end versions are shown on figure 2 left. The components used on these boards (linear and switched DC/DC regulators, ADC, ADC drivers and logic level shifters) have already been characterized under radiation by collaborators.

2.2 QIE10 front-end evaluation

A full prototype set-up was used for the first laboratory measurements with the QIE10 front-end. Due to unavailability of the CERN-VFC-HD board at the time of the tests, an Igloo2 development kit was used as back-end system. For complete operation, an SMA to SFP+ module and a custom clock conditioning circuit, including programmable delay lines, were attached to this kit.

On this prototype system, the front-end is continuously sampling and sending data to the back-end system in synchronism with an external 40 MHz clock (SPS/LHC bunch clock). When the back-end receives a trigger signal, the optical link data is temporally stored on a 512MB LPDDR memory using 64 bits words. The 64 bits data frames contain: bunch ID, Turn ID, data and

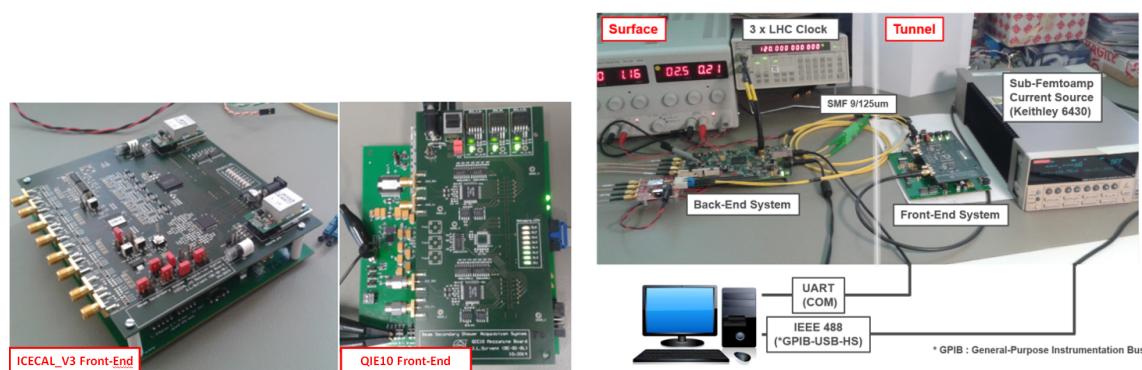


Figure 2. Front-End Prototypes (left) and setup for QIE10 Front-End evaluation (right).

status bits. This configuration allows the storage of 200ms of data at 40 MHz. A PC connected to the back-end system, through UART and with a custom user application, provides feedback on the optical link status, allows the user to perform the control of the front-end over the link and recovers the data from the LPDDR memory for analysis. This application also controls a Keithley 6430 sub-FemtoAmp current source through a general purpose instrumentation bus (GPIB). The complete set-up for laboratory tests is shown in figure 2 right.

QIE10 is a charge integrator and digitalizer ASIC able to cover a charge dynamic range of $1e5$ (17bits) with 8 bits encoding, this device also contains a 6 bits time-to-digital converter (TDC). The ASIC outputs the digital charge value and TDC information through eight double data rate (DDR) low-voltage differential signalling (LVDS) lines at 80Mbps. Its logarithmic charge encoding algorithm contains 16 sensitivity levels, which are divided in 4 ranges. The 8 bits encoded charge value consists of 6 bits for mantissa and 2 for range. The QIE10 uses 4 different internal capacitors (CID), to achieve integrations every 25 ns, with each integrator channel requiring 100 ns to process its 25 ns integral. In order to check the QIE10 response, logarithmic sweeps were performed with the Keithley current source. Temporal windows of 25 μ s (1000 samples at 40 MHz) were taken for each current increment, then, the integral value of each capacitor was averaged. The data measured was compared with the ASIC nominal logarithmic parametrisation to check any possible deviation, as shown in figure 3 left.

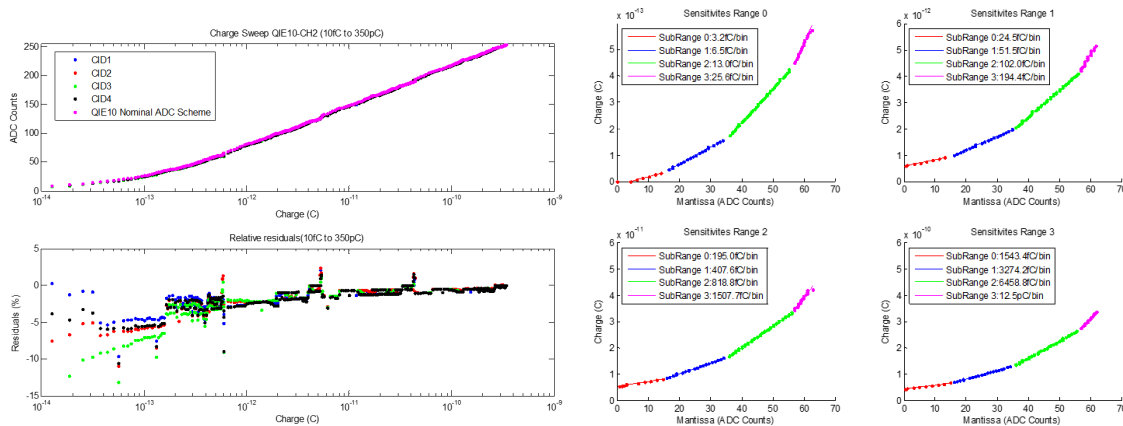


Figure 3. QIE10 response to a logarithmic current sweep (left) and sensitivity levels (right).

The top plot of figure 3, left, shows the QIE10 ADC values which represent the input charge, while the lower plot shows the residual error respect to the nominal response. It is clearly visible the logarithmic behaviour of the QIE10 and the 4 ranges in which the ASIC splits its dynamic range (seen as little spikes in the residual error). The measured values in our prototypes show a good agreement with respect to the ASIC nominal ADC response, remaining below 5% of difference, except for a small part of the first range. All the integrator capacitors show a similar response.

The check of the 16 sensitivity levels (4 per range) is shown in figure 3 right, plotting the charge versus mantissa value. The slope of the linear fits performed in each sub-range shows the sensitivity levels.

Both of the QIE10 ASICs contained on the front-end board show a similar behaviour, and the data collected during these studies can be used for calibration. The tests have shown that the

complete front-end performs according to specification, which qualifies the electronics in terms of functionality and accuracy for installation in the SPS tunnel for further testing. The TDC information is not required for the beam profile monitoring and therefore it is unused.

2.3 ICECAL_V3 front-end functional tests

ICECAL_V3 is a radiation-hard integrator ASIC, working at 40MHz, developed by the University of Barcelona for the LHCb experiment. It features 4 channels, with a charge sensitivity of 4fC and saturation at 16pC, featuring therefore a dynamic range of $4e3$. The ASIC provides an analog voltage every 25 ns proportional to the integrated current seen at the input. A linear 4 channel 12 bits ADC is responsible for the digitalization of the ICECAL outputs.

Very preliminary functional tests were performed on the ICECAL_V3 mezzanine to check that the conditioning circuitry and the ASIC itself were operational. A function generator AFG3252 was used to generate test pulses and the 40 MHz system clock. The system clock is connected to the back-end and recovered on the front-end through the optical link, the test pulse is attenuated and AC coupled to the readout ASIC input. Finally, the analog output is monitored with an AC coupled differential probe connected to a scope. The set-up and readout ASIC response is shown on figure 4. On the scope signal on figure 4, right, the system clock (blue), the input tests pulse (red) and the ICECAL response (green) are shown. The tests performed showed a correct operation of the ASIC, providing at its output a square pulse of an amplitude proportional to the integral value of the input pulse. Further analysis will be done on laboratory conditions before installation on the SPS tunnel.

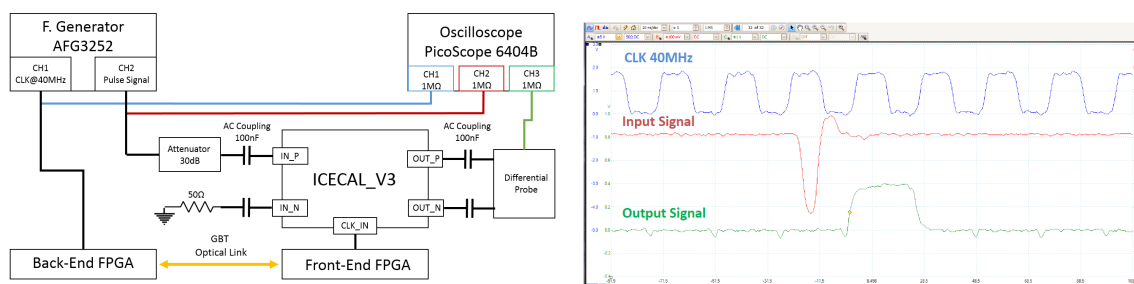


Figure 4. ICECAL_V3 mezzanine functional tests, setup (left) and signals (right).

3 System tests with beam wire scanners

3.1 SPS set-up

A set of four pCVD diamond detectors were installed on the Long Straight section 5 (LSS5) of the SPS accelerator at approximately 1.6m from an operational linear beam wire scanner (BWS51731). The aim of such set-up is to assess the performance of diamond detectors as beam profile monitors and evaluate the QIE10 front-end prototype for detectors readout. A nearby operational acquisition system, consisting on a scintillator attached to a photo-multiplier tube (PMT) and a pre-amplifier, is used for measurements comparison.

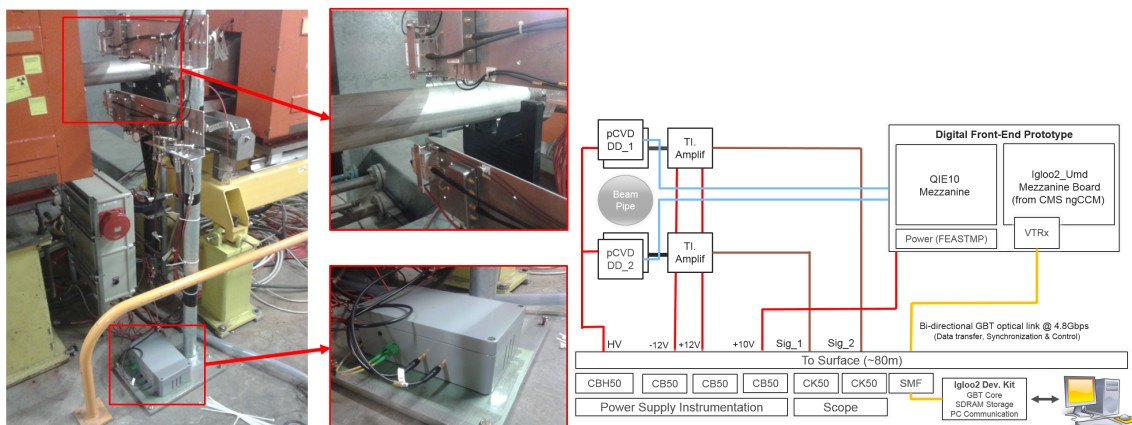


Figure 5. SPS Tunnel Set-up in detail (left) and connections schematics (right).

On this setup, two detectors are located on the top and two below of the beam pipe. One couple of top/bottom detectors is connected to transimpedance amplifiers, used to drive long CK50 ($\sim 80\text{m}$) cables up to the surface building. These current-to-voltage amplifiers are based on the THS3001 operational amplifier in transimpedance configuration, with a transfer function $V_o = 500I_d$, where I_d is the detector current and V_o the voltage seen on a 50Ω load. The other couple of top/bottom detectors are connected to the QIE10 Front-End prototype for its readout and digitalization. Such configuration allows to correlate the digital detector data, coming from the QIE10 Front-End prototype, with the analog data from the other set of detectors. The tunnel installation is shown on figure 5 left, and the connections schematics on the right.

On the surface, a LeCroy scope is used to acquire the analog data from the two detectors and scintillator system. The different tunnel electronics are powered from the surface, by using a Keithley 2410 to provide high voltage to the detectors ($\sim -500\text{V}$) and standard power supplies to deliver $+12/ - 12\text{v}$ for the amplifiers and 10V for the front-end prototype. The back-end prototype for digital data readout is the same as used previously on the QIE10 characterization, consisting of an Igloo2 FPGA development kit with the GBT core, SDRAM storage and PC communication. A SI5338 Evaluation board was used to provide the required 120MHz reference frequency for the Igloo2 Serializer/Deserializer, the SPS 40MHz bunch clock was used as clock input for the PLL. This configuration allows the optical link and the front-end acquisition electronics to be synchronized with the machine. Figure 6 shows the surface set-up (left) and a detailed view of the back-end prototype system (right).

3.2 Diamond detectors as beam profile monitors and QIE10 front-end performance

For the diamond detectors evaluation as beam profile monitors, a set of 4 scans were performed using the BWS51731-H linear beam wire scanner (BWS). To check diamond response at different beam intensities, the SPS accelerator was set-up with a LHC pilot beam at 450GeV . This beam consists on a single bunch in the accelerator with 4ns FWHM and a revolution period around $23\mu\text{s}$. The intensities used for the tests were $5.2\text{e}9$ and $1.1\text{e}11$ particles per bunch (PpB), two scans were performed for each intensity. During each scan, the signals from the analog part of the front-end, the scintillator/PMT pre-amplifier signal and the SPS turn clock were recorded with a LeCroy scope

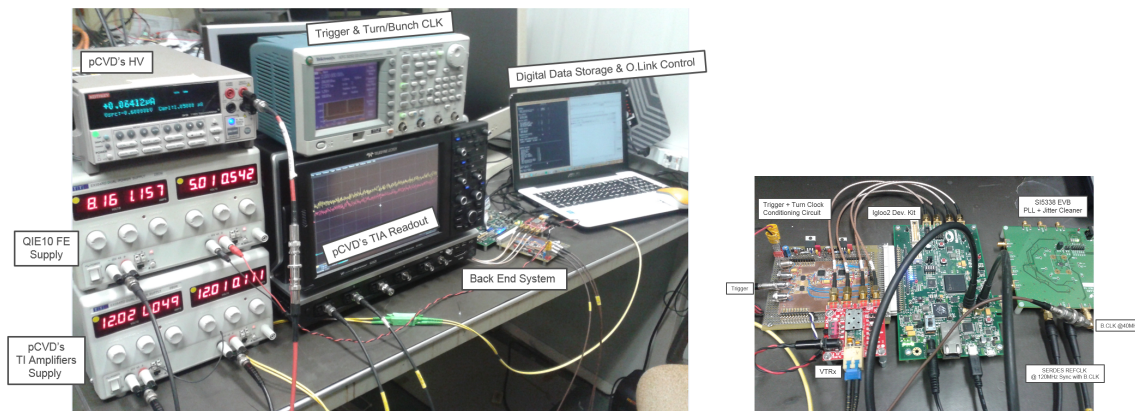


Figure 6. Surface Building setup (left) and back-end system in detail (right).

at 2.5GBPS. At the same time, the digital signal from the QIE10 front-end acquisition electronics was recorded on the Igloo2 development kit LPDDR SDRAM, and sent later to a computer for analysis. A trigger signal from the BWS motion control card was used for systems synchronization. Figure 7 shows a summary of the testing conditions.

Testing Conditions									
Scan Speed	HV for pCVD Diamonds	Carbon Wire Diameter	SPS USER	Bunches on Ring	Protons Per Bunch	Bunch Length (4 FWHM)	SPS Revolution Period	Energy	
1 m/s	-500 V	30 μ m	MD2 / LHC_Pilot	1	$5.2e9 \rightarrow 1.1e11$	4 ns	23 μ s	450GeV	

Figure 7. Testing conditions of the SPS accelerator, beam wire scanner and diamond detectors.

For the analog signal processing, a Matlab script was used to perform bunch integrals of 25ns once every turn around the only bunch on the accelerator, the SPS turn clock was used as temporal reference. Once the bunch integrals are extracted (charge), the data is normalized to be fitted with a Gaussian of amplitude 1. This normalization allows a direct comparison in terms of fitting quality between different beam profile sources for the same scan, studying the residuals and the sum of squared errors (SSE) of the fit. The scope memory only allowed to store IN or OUT scans at the specified sampling frequency.

With regard to the digital data from the QIE10 front-end system, the information on the back-end memory is recovered by a PC connected through a UART interface. On this case the beam profiles for IN and OUT scans were recorded. The digital data is transformed into its equivalent charge by using the QIE10 logarithmic nominal response as a look-up table for conversion. The front-end acquisitions at 40MHz were done on synchronization with the accelerator, therefore, there is a constant number of samples between different bunch integrals, corresponding to consecutive SPS revolution periods. For Gaussian fitting, normalization and parameters extraction, only the QIE10 points with the bunch integral value were considered.

The figure 8 shows the graphical report obtained processing the signals from the top and bottom detectors sampled with the oscilloscope (first two rows), the QIE10 Front-End data for the same scan (second two rows) and the PMT + Scintillator response (last row) for a beam wire scan performed with $5.2e9$ charges per bunch. Note that the pre-amplifier of the PMT was close to saturation and the beam shape shown is not a truly Gaussian profile.

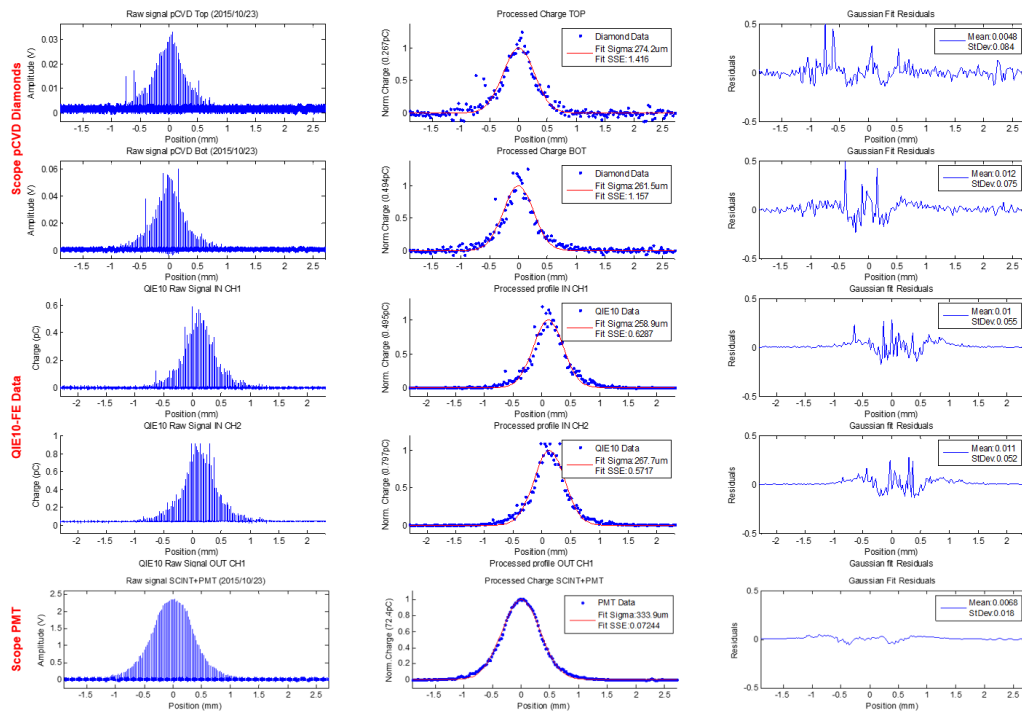


Figure 8. Beam profiles graphical reports with a SPS Pilot Beam 5.2e9 PpB at 450GeV.

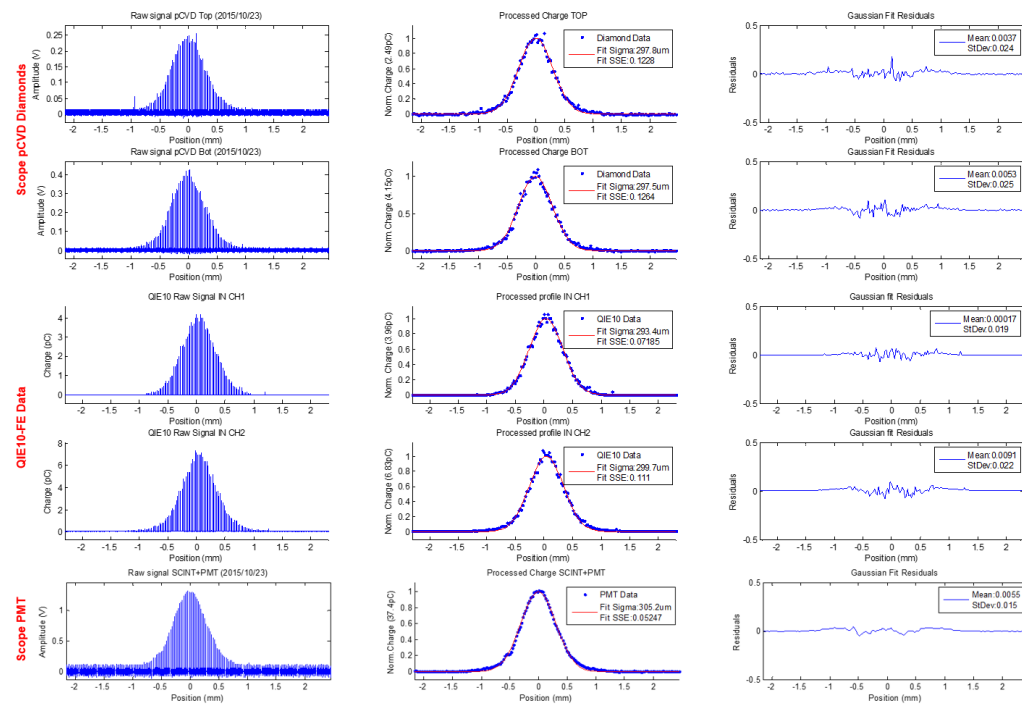


Figure 9. Beam profiles graphical reports with a SPS Pilot Beam 1.1e11 PpB at 450GeV.

Test summary: SPS Beam LHC_PILOT 5.2E9 PpB @ 450GeV										
	Sigma (um)			SSE (a.u)			Std.Dev. Residuals (a.u)			
	SCOPE	QIE10-IN	QIE10-OUT	SCOPE	QIE10-IN	QIE10-OUT	SCOPE	QIE10-IN	QIE10-OUT	
SCAN1	TOP	274.2	258.9	237.1	1.416	0.629	0.609	0.084	0.055	0.053
	BOTTOM	261.5	267.7	234.8	1.157	0.572	0.670	0.075	0.052	0.057
	COMBINED	267.7	x	x	0.876	x	x	0.066	x	x
	PMT	333.9	x	x	0.072	x	x	0.018	x	x
SCAN2	TOP	219.3	210.5	x	0.653	0.511	x	0.057	0.049	x
	BOTTOM	230.2	224.1	x	0.409	0.305	x	0.044	0.038	x
	COMBINED	225.1	x	x	0.345	x	x	0.041	x	x
	PMT	306.4	x	x	0.067	x	x	0.017	x	x

Test summary: SPS Beam LHC_PILOT 1E11 PpB @ 450GeV										
	Sigma (um)			SSE (a.u)			Std.Dev. Residuals (a.u)			
	SCOPE	QIE10-IN	QIE10-OUT	SCOPE	QIE10-IN	QIE10-OUT	SCOPE	QIE10-IN	QIE10-OUT	
SCAN1	TOP	297.8	293.4	284	0.123	0.072	0.062	0.024	0.019	0.018
	BOTTOM	297.5	299.7	295.1	0.126	0.111	0.112	0.025	0.022	0.022
	COMBINED	297.7	x	x	0.086	x	x	0.02	x	x
	PMT	305.2	x	x	0.052	x	x	0.015	x	x
SCAN2	TOP	319.6	319.3	310	0.101	0.081	0.061	0.022	0.02	0.017
	BOTTOM	320.4	317.7	314	0.083	0.067	0.075	0.02	0.018	0.019
	COMBINED	320	x	x	0.058	x	x	0.017	x	x
	PMT	327.7	x	x	0.027	x	x	0.012	x	x

Figure 10. Summary of beam profile measurement with diamond detectors and QIE10-Front-end.

From the detector comparison point of view, the scintillator and PMT assembly is showing a much cleaner distribution whereas the diamond detectors show spiky profiles. Very little improvement was reached when combining the two diamond detectors measurements. The spiky profiles obtained on the diamond detectors, with such low beam intensity, could be explained as a direct relationship between the effective area of the detectors and the random distribution nature of the secondary particles cone. Each diamond detector has an effective area of 1 cm^2 ($1 \times 1 \text{ cm}$) whereas the scintillator is around 100 cm^2 ($10 \times 10 \text{ cm}$), therefore, the bigger the detector the smaller the statistical error for a random shower of secondary particles.

Concerning to the data acquired on the tunnel with the QIE10 front-end, the profiles of both detectors are showing the same spiky behaviour. However a clear improvement on noise reduction can be observed, especially on the tails of the gaussian fit and on the residuals. The noise reduction is translated on better accuracy on tails measurement and better gaussian goodness-of-fit, having a lower sum of squared errors (SSE) and residuals standard deviation than the profiles seen on surface. The same analysis approach was used for the beam profiles acquired with a higher beam intensity ($1.1e11$ charges per bunch), see figure 9.

With an increase in beam intensity, the amplitude of the detectors signal is increased, and the statistical fluctuations seen on the diamonds signals (spikes) are much lower compared with the gaussian amplitude. On this case, the performance between the operational system and the diamonds is comparable, the gaussian fitting quality of the scintillator and PMT data is a factor two better (see SSE and residuals). However, taking into account the effective area ratio diamonds/scintillator $\sim 1:100$, the diamonds are showing a good performance for beam profile monitoring. As previously, the secondary particle shower was acquired with the QIE10 front-end on the tunnel (second two rows), these profiles are showing similar characteristics to the scope recorded signals, and again, an improvement can be observed in terms of noise (visible on the gaussian tails). The logarithmic encoding and its 1% constant quantification error do not degrade the quality of the gaussian fit.

The tables of figure 10 show a numeric summary of the processed parameters extracted from the different scans. It is possible to see numerically the improvement on the diamond profiles (Top/Bottom in scope) due to beam intensity increase checking the SSE (sum of squares errors) and the Std.Dev.Residuals (standard deviation of the residuals). The performance of the QIE10 acquisitions on the tunnel (QIE10-IN/OUT) is also detailed, and in comparison with the scope signals for top and bottom detectors, tunnel acquisitions feature a lower SSE and residuals for each specific scan.

4 Conclusions

The first complete secondary particle acquisition system prototype, based on the QIE10 readout chip, has shown an excellent performance under operational conditions. The system is easy to operate and no tuneable parameters were needed to measure different beam intensities. The QIE10 ASIC has demonstrated to be a suitable candidate for diamond detector readout.

With regard to the pCVD diamond detectors, they are reliable detectors for beam profile monitoring. However, its performance, due to its small cross-section, is related not only on the placement respect to the beam/wire interaction point, but also on the machine beam characteristics, such as the proton beam intensity and energy. Further statistical studies are required to understand the impact of these different parameters and optimize the diamond detectors placement by means of simulations. For the specific location of our set-up and for a beam intensity $1e11$ particles per bunch at 450GeV, the diamond profiles are showing a comparable performance to the current operational systems consisting on a big scintillator attached to a photomultiplier.

References

- [1] B. Dehning, A. Guerrero, T. Kroyer, M. Meyer and M. Sapinski, *Carbon fiber damage in particle beam*, in the proceedings of the *46th ICFA Advanced Beam Dynamics Workshop on High-Intensity and High-Brightness Hadron Beams*, Morschach, Switzerland, September 27–October 1 2010, pp. 231–234 and online at <http://jacow.org/>.
- [2] J. Emery et al., *A fast and accurate wire scanner instrument for the CERN accelerators to cope with high environmental constraints and increasing availability demand*, in the proceedings of the *2014 IEEE Conference on Controls Applications (CCA)*, Antibes, France, October 8–10 2014, [IEEE](#) (2014), pp. 1139–1145.
- [3] M. Kuhn et al., *Investigations of the LHC emittance blow-up during the 2012 proton run*, in the proceedings of the *4th International Particle Accelerator Conference (IPAC 2013)*, Shanghai, China, May 12–17 2013, pp. 1394–1396 and online at <http://jacow.org/>.
- [4] J.L. Sirvent, B. Dehning, J. Emery and A. Diéguez, *Secondary particle acquisition system for the CERN beam wire scanners upgrade*, [2015 JINST 10 C04021](#).
- [5] P. Moreira et al., *The GBT Project*, in *Topical Workshop on Electronics for Particle Physics*, Paris, France, September 21–25 2009, <http://dx.doi.org/10.5170/CERN-2009-006.342> and online pdf version at <https://cds.cern.ch/record/1235836/files/p342.pdf>.
- [6] *VME FMC Carrier HPC-DDR3 (VFC-HD)*, <http://www.ohwr.org/projects/vfc-hd/wiki>.
- [7] E. Picatoste et al., *Low noise 4-channel front end ASIC with on-chip DLL for the upgrade of the LHCb Calorimeter*, [2015 JINST 10 C04017](#).
- [8] A. Baumbaugh et al., *QIE10: a new front-end custom integrated circuit for high-rate experiments*, [2014 JINST 9 C01062](#).
- [9] *The Igloo2 UMD Board Specifications*, <https://cms-docdb.cern.ch/cgi-bin/PublicDocDB/ShowDocument?docid=12596>.
- [10] M. Barros et al., *The GBT-Based Expandable Front-End (GEFE)*, in *The GEFE project @ TWEPP15*, Lisbon, Portugal, September 28–October 15 2015.